Review

Progress of Organic/Inorganic Luminescent Materials for Optical Wireless Communication Systems

Javier Martínez [ID], Igor Osorio-Roman *[ID] and Andrés F. Gualdrón-Reyes *[ID]

Facultad de Ciencias, Instituto de Ciencias Químicas, Isla Teja, Universidad Austral de Chile,
Valdivia 5090000, Chile; javier.martinez@uach.cl
* Correspondence: igor.osorio@uach.cl (I.O.-R.); andres.gualdron@uach.cl (A.F.G.-R.)

Abstract: The growing demand for faster data transference and communication allowed the development of faster and more efficient communication network-based technologies, with wider bandwidth capability, high resilience to electromagnetic radiation, and low latency for information travelling. To provide a suitable alternative to satisfy data transmission and consumption demand, wireless systems were established after a decade of studies on this topic. More recently, visible light communication (VLC) processes were incorporated as interesting wireless approaches that make use of a wide frequency communication spectrum to reach higher bandwidth values and accelerate the speed of data/information transmission. For this aim, light converters, such as phosphor materials, are reported to efficiently convert blue light into green, yellow, and red emissions; however, long carrier lifetimes are achieved to enlarge the frequency bandwidth, thereby delaying the data transference rate. In this review, we focused on recent advances using different luminescent materials based on prominent polymers, organic molecules, and semiconductor nanocrystals with improved photophysical properties and favored carrier recombination dynamics, which are suitable to enhance the VLC process. Here, the main features of the above materials are highlighted, providing a perspective on the use of luminescent systems for efficient optical communication applications.

Keywords: luminescent materials; visible light communication; optical properties; radiative recombination; light conversion

1. Introduction

With the purpose of ensuring the increase in the speed of both data transmission and consumption, advanced strategies were previously studied to overcome the limitations imposed by using radio-frequency technology, establishing efficient optical communication approaches, such as wireless network systems [1,2]. Among the most prominent alternatives used to accelerate information transference, visible light communication (VLC) is highlighted due to its use of solid-state light (SSL) converters, enabling access to a wide bandwidth in the scale of THz [3,4]. This fact allows users to carry out wireless communication across the electromagnetic spectrum from UV to NIR [4]. One of the main light sources for VLC is based on light-emitting diodes (LEDs), where a phosphor-based active layer is incorporated into a device to absorb the blue light coming from a commercial component, usually InGaN, and re-emits illumination at larger wavelengths [5–7]. This configuration produces luminescent white color LEDs (WLEDs) with high color purity and an improved color rendering index (CRI) [8–10], facilitating the development and subsequent commercialization of LEDs-based technologies, such as lighting systems, LCD displays, organic-LEDs (OLEDs), etc.

As seen Figure 1, VLC systems are generally based on light link between a blue-emitting LED, a luminescent active layer, and a photodiode. The composed LED device, which produces the illumination, is named the emitter subsystem, while the photodiode, which receives the signal coming from the LED, is known as the receiver subsystem [11].

Next, the emitter obtains the signal from a signal generator, which imposes a bias current to drive the LED. Here, the signal that reaches the LED (known as the original binary response) is previously transformed through encoding, modulation, and pre-equalization processes, before being converted into a digital signal to modulate the light intensity of the emitting device [12]. The LED into the VLC system must work continuously while the data are transmitted, and, simultaneously, the power stage ensures that the emitted light serves as a continuous illumination source. At this point, the electrical signals are transformed into an optical response, which contains all the information through its frequency [13]. Clearly, the frequency bandwidth will depend on the intrinsic properties of the luminescent material employed as the active layer, and commonly, a long-pass optical filter is introduced to filter out the remanent blue-light emitted by the LED. After the light transmission step, the optical signal is collected through the optical lens (transmitter and receiver ones, Tx and Rx, respectively) with the purpose of enhancing the signal strength to reach the photodiode and extend the transmission distance [13]. Interestingly, the modulated light can travel through open spaces, such as air or water. Lastly, the photodiode perceives the optical signal (also called the original transmission response), transforming it into an electrical response, and treats it under the post-equalization, demodulation, and decoding processes to obtain the desired digital signal [11].
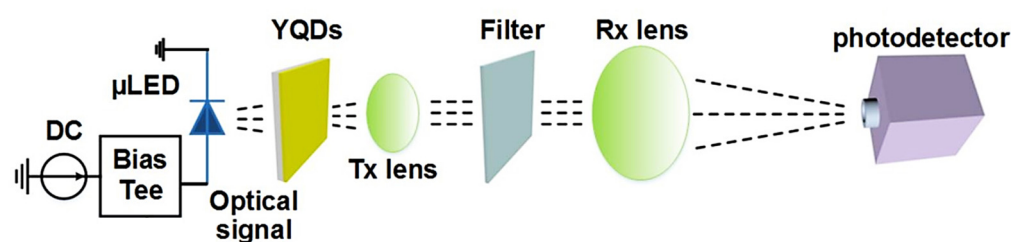
Figure 1. Schematic representation of a typical VLC system: luminescent active layer (for instance, yellow-emitting quantum dots) on a blue-light LED transmitting optical signals to reach Tx and Rx lens, as well as introducing long-pass filter to suppress remanent blue-light coming from illumination source. Optical response is collected by photodetector to produce an electrical response related to function of quality of data transmission. Reproduced and modified with permission [13]. Copyright 2018, American Chemical Society.

One of the most useful SSL converters is based on yellow phosphors, such as $Y_3Al_5O_{12}$:Ce^{3+} (YAG:Ce), providing high performance and brightness to the WLEDs; however, this luminescent species shows a long excited state lifetime (in the microscale range) [14–16]. This intrinsic characteristic only favors the accessibility to a bandwidth of a few MHz, restricting the frequency modulation and, thereby, limiting the speed of the wireless communication [17]. To overcome these drawbacks, several strategies were applied, such as (i) the optimization of the LED structure, where the resistance and capacitance of the device components are reduced to accelerate the carrier recombination dynamics [18,19]; and (ii) the blue-filtering process [20,21], which is pivotal to suppressing the parasite signals produced by phosphor emitters. Unfortunately, these enhancements extended the modulation bandwidth by ~30 MHz, which is insufficient for VLC [7]. Thus, it is deductible that novel materials for light conversion with faster radiative recombination, high brightness, and notable optical features are needed to strengthen the wireless communication technologies.

In this quest, some organic semiconductors, such as oligofluorenes [4,22] or composed polymers [23], were employed as light converters for VLC due to their low-energy band gap (yellow emission), high photoluminescence quantum yield (PLQY), fast radiative recombination lifetimes, and facile integration with commercial blue-emitting nitride-based LEDs. Under this premise, two-color white light emission can be produced, for instance, for VLC datalink applications [17]. However, CRI values of ~57% are obtained, indicating the difficulty of obtaining a stable and high color purity in the white color tonality [7].

Therefore, the preparation of light converters based on green- and red-PL emission is primordial to combination with blue-LEDs, extending the broadband luminescence of the final device to increase the CRI. More specifically, among the red-emissive organic tools with high PLQY and favored radiative recombination rates, the actual state-of-the-art elements are limited to show high-quality blue-light emitters with the strong optical power required to generate a suitable signal-to-noise ratio for the modulation of bandwidth in VLC. In conclusion, research groups are focused on the preparation of green-light emission-based converters, which can absorb the blue-light from the LEDs. This process allows access to low wavelengths from the visible spectrum, transferring carriers to red-light emitters to cover a wider energy spectrum, including red-IR range [22].

In this review, we exhibit the recent progress of promising luminescent materials with valuable photophysical properties, highlighting organic polymers, organic semiconductors, metal-organic framework/mixed matrix membranes, and semiconductor-based nanocrystals with high optical performance. We provide new insight about how the intrinsic features of these materials could be tuned to promote improvements in the CRI and color quality of WLED, OLEDs, and other prominent devices, providing a step forward to facilitate more efficient data/information transfer from optical wireless technologies.

2. Luminescent Materials for VLC Systems

2.1. Metal Organic Frameworks (MOFs)

Recently, the scientific community focused its efforts on the design of novel materials which show luminescence functionality with applicability in areas such as OLEDs, luminescence-based sensors, etc. They present very interesting properties in the application of functional electronic/optical devices, since these compounds exhibit outstanding mechanical and electronic features; these materials are known as MOFs [24,25]. MOFs are hybrid inorganic–organic crystalline materials that consist of a union between metal ions and one or more organic bridging ligands with different components and coordination modes. This fact means that MOFs display applications in a considerable variety of fields [24].

A MOF-based material with potential applicability in VLC and light-emitting devices was designed by Chen et al. [26], by whom the encapsulation of rhodamine was performed in an adenine-based bio-MOF. The authors realized that an increment in rhodamine concentration permitted color emissions from green to red, with emission lifetimes ranging from 3 to 7 ns. Here, the best CRI value of ~94% was obtained using the material based on bio–MOF, BSSO, Rh@bioMOF–1, and CASN [BSSO–$(Ba,Sr)_2SiO_4:Eu^{2+}$, CASN–$CaAlSiN_3:Eu^{2+}$] [26]. Then, the possible use of dye-encapsulated MOFs in OLEDs was evaluated with a rhodamine–B/aluminum–MOF system (Al–DBA MOF). The combination of emissions from the dye (yellow) and linker (blue) allowed the fabrication of a WLED, which was known as MOF–WLED, exhibiting a frequency bandwidth of 3.6 MHz and a data rate of 3.6 Mbps [27]. Recently, a zeolitic imidazolate framework nanocrystal (PAN@ZIF–8) was also synthesized and successfully used as a self-powered VLC system for wireless human–machine interactions [28]. Additionally, mixed-matrix membranes (MMMs) based on luminescent MOFs and emissive polymers were proved in high-speed VLC. For instance, Mohammed et al. [29] exhibited the preparation of MMMs based on the combination of emissive and stable zirconium-based MOF (NU–1000) and a luminescent PIM–1 (denominated as polymers of intrinsic microporosity–1), where an efficient energy transfer from the MOF to the polymer was promoted. The corresponding structures of the Zr–MOF and the polymer are shown in Figure 2a. The resultant MMMs revealed an exceptional modulation bandwidth of ~80 MHz, affording a light communication rate of 215 Mbps, which represents a significant increase compared to the value displayed using the pure polymer (132 Mbps), as shown in Figure 2b. On the other hand, a promising luminescent MOF based on $Zn_2(tcbpe)$ (H_4tcbpe = 1,1,2,2-tetrakis(4-(4-carboxyphenyl)phenyl)ethene) were shown to be an efficient converter of blue-light to yellow emission, using PLQY ~76%, which can be improved by changing some of the organic ligands linked to the central

metal with fluorinated tools [30]. Here, a PLQY of ~88% can be achieved, with this rate being the actual record for yellow-emitting, blue-excitable MOF phosphors. At this point, the introduction of fluor into the main MOF structure produces a redshift in the optical properties, mainly in PL emission, and accelerates the radiative recombination pathway, generating lifetimes between 2 and 4 ns. Next, porous Zn-MOFs crystals based on benzenedicarboxylic and triethylenediamine were synthesized, with rhodamine molecules being encapsulated, thus producing warm-yellow emission with a PL lifetime of ~6 ns [31]. Even if it is not reported, for any configuration of a VLC system for these types of MOFs, the deposition of the luminescent material on blue-LED to generate white emission with high color purity in function of the density of the added halide or the luminescent molecule could provide a novel alternative to accelerate data transmission. Lastly, as the-state-of-the-art developments in the use of MOFs in VLC are limited, this issue presents an interesting starting point for the innovation regarding the development of diverse MOFs structures (metal/ligand nature and stoichiometry) and production of potential light converters for fast wireless communication.
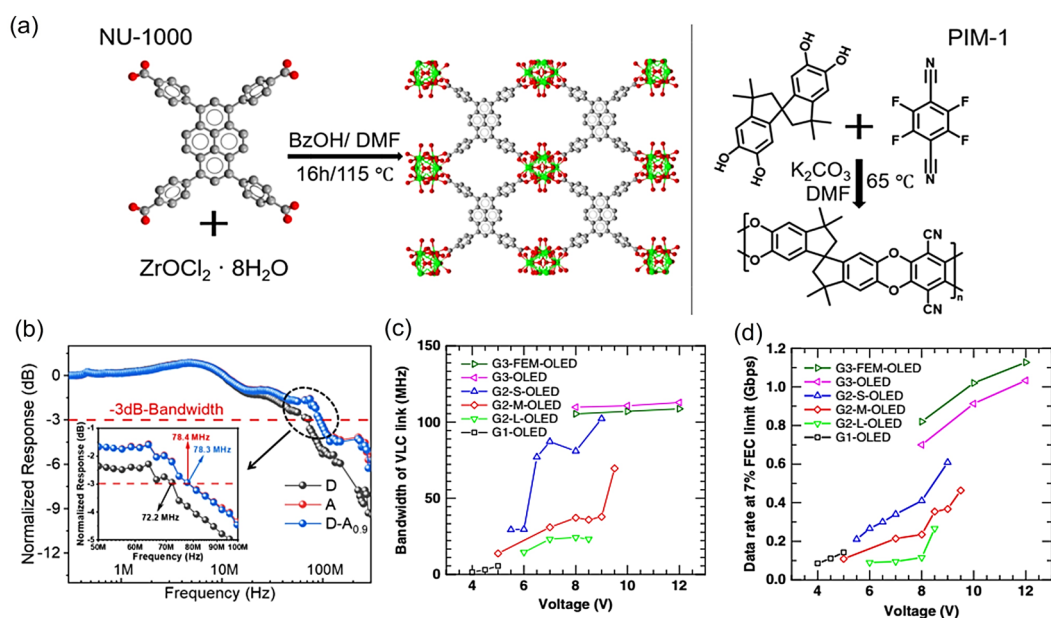
Figure 2. (**a**) Schematic illustration depicting synthetic conditions required to obtain typical molecular structures of Zr–MOF (NU–1000) and PIM–1. (**b**) Frequency response measurements for NU–1000/PIM–1 MMMs (where D is associated with MOF as donor, A is ascribed to PIM–1 as acceptor, and D–A0.9 is donor–acceptor assembly with a 90 wt% A). Reproduced with permission [29]. Copyright 2022, American Chemical Society. (**c**) Frequency response measurements and (**d**) data rate (7% forward error correction limit) of diverse OLEDs by varying transporting layer (diverse generation, G, and sizes) between OLEDs in function of operational voltage. Reproduced under terms of CC-BY license [32]. Copyright 2020, Authors, Springer Nature.

2.2. Organic Molecules–Organic-Light Emitting Diodes (OLEDs) in VLC

Recently, by addressing advantages in material science and fabrication processes, solid-state devices, such as OLEDs, were gradually implemented in various small and medium displays. However, the fastest VLC systems reported so far make use of optical transmitters, which consist of LEDs [22,33] and laser diodes (LDs) [33–35] and feature inorganic semiconductors (typically gallium nitride) as the emissive medium. This characteristic affords high optical output power and broad bandwidth, deducing that inorganic LEDs [36,37] and LDs [38,39] are suitable for integration into a dual system capable of simultaneously providing white lighting and fast data transmission. However, the use of

OLEDs represents a valid alternative, which gained considerable attention for VLC in the last few years [40–45].

In the literature, different types of OLEDs were proposed for VLC (named as OLED-based VLC, OVLC), with studies concluding that the performance of the OLEDs is defined by the properties of the luminescent organic molecules for this application. However, the organic devices are hampered by scenarios in which there is a low level of visible light penetration in non-transparent media. The suitable solution found by research groups is related to extending the communication system operations to the "almost (in)visible" region of the near-infrared (NIR, 700–1000 nm) using a new OLED type based on Pt(II) and Ir(III) complexes, modified porphyrins, donor-acceptor copolymers, small molecules-polymer blends [46,47], etc. However, OLEDs have a low modulation bandwidth (hundreds of kHz) compared to their analogous inorganic LEDs (typically several MHz). This fact is mainly attributed to the restrained charge carrier mobility in the organic semiconductors, limiting the applicability of the organic devices [46–49]. In this context, equalization processes (supply a higher charging voltage to the device for improving the carrier transport) [50] were applied to OLEDs, with one study obtaining a frequency bandwidth up to 10 MHz and a datalink supporting up to 100 Mbps [51]. This performance could be the initial step in the process of fabricating efficient OVLC systems.

Recently, small organic molecules were employed as optoelectronic components in VLC [52]. It is known that organic devices present several advantages compared to the inorganic ones, since these devices offer lower heat dissipation, reduced production cost, and wide photoactive areas. However, it is quite difficult to replace inorganic devices with organic devices because the former types dominate the current market [53]. The first electroluminescent device based on OLEDs containing small organic molecules was reported by Tang and VanSlyke, which was known as SMOLEDs [54]; later, an important number of improved OVLCs were developed using organic photonic devices as the device's transmitter, the receiver, or both components [55,56]. In addition, organic photodiodes (OPDs) could be seen as future devices for image sensor-based applications and optical communications because of their elevated sensitivity and superior responsivities [57]. This assumption is true in the case of OPDs containing active layers, such as bathocuproine (BCP) doped with 3,4,9,10-perylenetetracarboxylic bis-benzimidazole (PTCBI), which provides high values of bandwidths (~430 MHz) [58]. Other examples of OPDs are based on active layers containing donor species, as is the case for donor–π–acceptor selenophene (composed by heterocyclic units) devices with acceptor molecules, such as fullerene [59]. Through the fabrication of bulk and planar donor-acceptor heterojunctions to facilitate the carrier transport and increase as much as possible the photoresponsivity in the OPD, maximum values of frequency bandwidth and real-time data rate were estimated to be 1.4 MHz and 150 Mbps, respectively.

The principal inconvenient factor for a majority of organic devices is related to their low bandwidth (<1 MHz); thus, most of recent studies focused their efforts on the design of OVLCs with higher data transference rates [23]. For example, an OVLC based on organic semiconductors, such as polypara-phenyl vinylene copolymer, reported by Chun and coworkers [17] afforded a bandwidth of more than 200 MHz, although this bandwidth was limited by the other components in the system (the excitation source and the detector). Furthermore, they achieved a 1.68 Gbps data rate, which was an excellent result for white-light VLC link. Other OLED devices were able to achieve bandwidths of ~245 MHz with data rates beyond 1 Gbps, as shown in Figure 2c,d, respectively, making them excellent organic materials for VLC applications [32]. At this point, these types of OLEDs can br fabricated by adding a conventional luminescent emitter based on 2,5,8,11-tetra-tert-butylperylene (TBPe) and a fast emission molecule (FEM), such as 4,4′-bis [4-(diphenylamino)styryl]biphenyl (BDAVBi). Moreover, different generations (G) of device structure (1, 2 and 3) and the sizes (denoted as S, M and L) of the active areas were compared, with the best performance achieved for G3-FEM-OLEDs. It is important to recognize that OVLC has a set of limitations, since there is a shortage of commercially available organic devices, and these systems

recently emerged as promising materials in this area. In this way, it is deductible that these materials were not prepared at industrial quantities.

2.3. Polymers

After discovering luminescent properties in polymers, some investigations focused their efforts on improving the light output, lifespan, and power efficiency of polymers introduced in diode-based device structures [60–62]. This notion is the case for another type of OLED devices containing organic electroluminescent polymers, which are known as PLEDs, that were previously reported by Burroughes et al. [60]. In this context, the principal difference between SMOLEDs and PLEDs is the processing method. PLEDs are more related to solution processing, whereas SMOLEDs are commonly based on thermal-vacuum evaporation. Thus, it would be desirable to use the PLED processing method because it is cheaper. Next, it is important to highlight that polymer optical fibers, such as PLEDs, present a set of advantages compared to copper cables, glass fibers, and wireless communication systems, since these materials grant excellent properties, such as high fracture toughness, elevated elastic strain limits, electromagnetic interference, etc. [45]. In this line, Haigh et al. [49] reported transmission speeds of 10 Mbps using a PLED based on luminescent poly[2-methoxy-5-(3′,7′-dimethyloctyloxy)-1,4-phenylenevinylene] (MDMO-PPV), demonstrating the potential of polymers in the VLC area. On the other hand, a fast color converter was designed using a blend of conjugated polymers based on poly[2,5-bis(2′,5′-bis(2″- ethylhexyloxy)phenyl)-p-phenylenevinylene] (BBEHP-PPV) and poly[2-methoxy-5-(2′-ethyl-hexyloxy)-1,4-phenylene-vinylene] (MEH-PPV), in which there was a color change from green to orange–red. This feature allowed us to reach a modulation bandwidth value of ~200 MHz with a data rate of 350 Mbps [7]. More recently, a set of interesting PLEDs materials with potential applicability in VLC system were reported [22,63–65]. Some examples of these types of materials are related to emissive π-expanded diketopyrrolopyrrole dyes, 1-mm core size polymethyl methacrylate (PMMA), P3HT and PTB7 polymers, and polycarbonate multicore polymers, which were even studied in 5G VLC telecommunication systems. In general, advances in OLEDs devices are still under study in regard to their application in VLC, despite the disadvantages that organic active layers present. This point can be widely analyzed by observing the most prominent organic structures that have good electronic properties (i.e., prone to facilitate the carrier mobility) and produce efficient light conversion [23,52].

2.4. Features of BODIPY Dyes

The organic system known as BODIPY is a class of luminescent dyes that is extensively used in VLC scenarios. BODIPY dye is typically incorporated into a polymeric film, which is then used as a filter or coating on a light source, such as a LED. The dye absorbs light from the LED and re-emits it at a different wavelength [66], which can then be detected via a photodetector to create a VLC system. In particular, BODIPY dyes are attractive for VLCs due to their high photostability, high quantum yield, and narrow emission spectra [66,67]. In this context, Sajjad et al. [4] reported two different families of oligofluorene-BODIPY materials as alternative materials for color conversion in VLC, such as Y- and T-type, as shown in Figure 3a. Steady-state measurements of BODIPY show that the photophysical properties, including absorption and emission, can be tuned by controlling the molecular shape and lengths of the fluorene arms, and all the materials in solid state are highly emissive, with PLQY ranging from 55% to 75%, making them suitable for light-emitting devices and VLC.

The emission lifetimes show that all BODIPYs' lifetimes, as shown in Figure 3b,b', are much shorter (3.36–5.22 ns) than those of conventional phosphor color converters (µs scale) [68], while modulation studies show that BODIPYs have an order of magnitude higher modulation bandwidth (~39 MHz) and data rate (~100 Mbps) than the commercially available phosphor-based LEDs for VLC, as shown in Figure 3c. In this sense, other authors agree with the notion that the BODIPY system was proven suitable for VLC

applications during the past eight years [69,70], giving a maximum frequency of up to 73 MHz and date rate of 370 Mbps. BODIPY species in polydimethylsiloxane matrix were used as color conversion layers over blue LED to produce white light with CRI of 95% and CCT of 4200 K [71]. On the other hand, new OLEDs based on BODIPY (with different aromatic substitutes) and diverse mixtures with PMMA showed promising results for use in OLEDs due to their high stability, brightness, and color tunability resulting from their characteristic electroluminescence (EL) spectra, as shown in Figure 3d [72]. For PLQY, ~87–95% was obtained, with a frequency bandwidth of 55 MHz and a data rate of 218 Mpbs. It is deductible that a high PLQY is crucial to achieve an improvement in the VLC system. Thus, BODIPY elements are an attractive option for use in various optoelectronic applications [71,73–75]. Overall, BODIPY dyes offer a promising solution for VLC systems, as they can provide secure data transmission without interfering with other wireless communication systems.
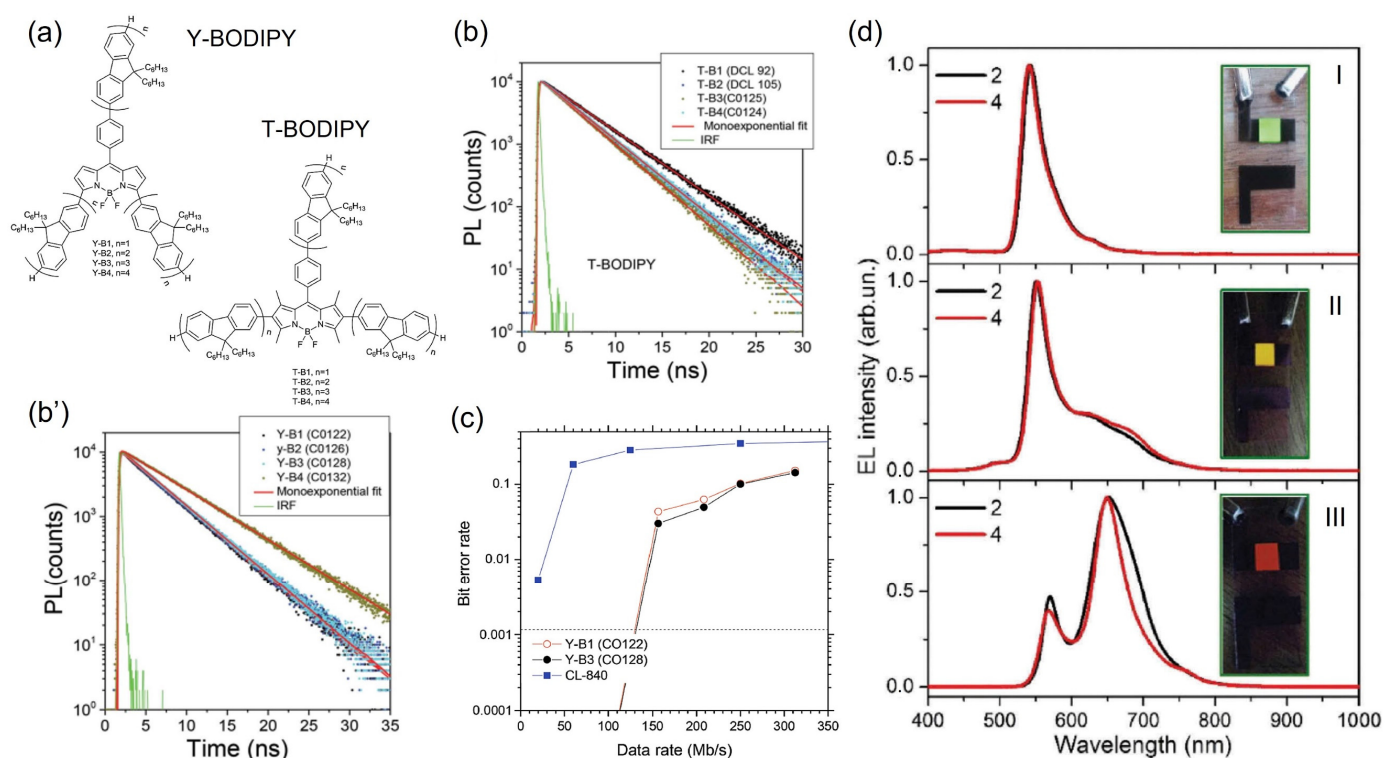
Figure 3. (**a**) Typical structures and PL lifetimes of (**b**) Y–BODIPY– and (**b'**) T–BODIPY–based molecules under different n-repetitions of oligofluorene arms. (**c**) BERs measurements by varying data rate for Y–BOPIPY (n = 1, 3) system, compared with a commercial phosphor color converter CL–840. Reproduced under terms of CC–BY license [4]. Copyright 2015, Authors. John Wiley and Sons, Inc. (**d**) EL spectra of OLEDs based on BODIPY doping on PMMA matrix: (I, green) 5% doped, (II, yellow) 10% doped, and (III, red) 100% emissive organic layer. Black and red curves indicate use of BODIPY with naphthalene and pyrene substitutes in its main structure, respectively. Reproduced with permission [72]. Copyright 2017, Elsevier.

2.5. Halide Perovskite Nanocrystals

Given the outstanding intrinsic properties of perovskite nanocrystals (PNCs), such as their high absorption coefficient [76], modulable band gap generated via quantum confinement effect or composition engineering [77,78], labile surface chemistry [79], and facile synthesis [80], these materials attracted growing interest in hot-research fields, such as optoelectronic and photovoltaics. PNCs unlocked high efficiencies in multicolor LEDs, with EQE up to 28% [81], while competitive PNCs-based solar cells achieved values closer to the records for the perovskite technology [82]. Most importantly, the PLQY of PNCs can

achieve values up to 100%, indicating the high quality and color purity of these systems [83]. This performance is associated with a lowered defect crystalline structure covered by a suitable density of capping ligands for material stabilization, suppressing the non-radiative carrier traps and promoting the radiative PL dynamics. However, unlike the chalcogenide-based nanocrystals, PNCs display color instability caused by the emergence of surface defects due to the eventual loss of capping ligands through aging time [84], as well as halide exchange reactions when PNCs with different halide natures are combined [85,86]. Therefore, even perovskite mixtures can offer a high PLQY and CRI values of >80% during the generation of white emission, while the PLQY of the final combination is <70% [87,88]. Additionally, red-emitting PNCs based mainly on $CsPbI_3$ are reported to be vulnerable to the presence of oxygen, humidity, and illumination conditions, inducing fast quenching of their optical features [89]. To overcome these issues, Mora-Seró et al. [90] showed that the combination of carbon quantum dots (CQDs) with $CsPbI_3$ PNCs (Red light-converter) prepared via a modified synthetic route can prolong their chemical stability for more than 1 year. Here, CQDs produce a broad PL, covering the blue/green range from the visible spectrum (green/blue-light converter). By fixing a constant concentration of CQDs ($10 \, mgmL^{-1}$) and adding different concentrations of $CsPbI_3$ PNCs (described as 10-CQDs-X-PNCs), they were able to modulate the white light tonality from cold to warm white emission, as shown in Figure 4a,b. The maximum PLQY of the CQDs-PNCs combination was 75%, and this composite material was used as an active layer for WLEDs, providing a CRI ~95%, as shown in Figure 4c. This result indicates an improvement in the white color quality of the device. For this reason, PNCs are considered convenient light converters for VLC [91,92].

The enhancement of the CRI for white light emission coming from CQDs and PNCs active layers is in line with the typical CRI value of ~89% established by Bakr et al. [8], who introduced $CsPbBr_3$ PNCs, combined with commercial red-emitting phosphors, to generate warm-white light tonality. By exhibiting a PLQY of ~70% and a fast radiative recombination pathway for carrier relaxation into the nanocrystals (7.0 ± 0.3 ns), the composite light converter provides a high frequency bandwidth of 491.4 MHz, covering a wider electromagnetic spectrum than YAG-based phosphors (3–12 MHz), nitride-based active layers (~12.4 MHz), and organic molecules-based light converters (40–200 MHz) (Figure 4d). On the other hand, through bit error rate (BERs) measurements, $CsPbBr_3$ PNCs-red phosphor-based light converters can transmit data at 2 Gbps, which is a record in VLC applications. Despite the authors reporting the intrinsic stability of the PNCs in ambient air, it is well known that O_2 and humidity can progressively damage the perovskite structure, altering their integrity and, therefore, quenching their photophysical features.

By introducing the concept of anion-exchange into the PNCs (interchange in bromide and iodide domains into the nanoparticle structure), mixed halide PNCs were prepared [93], with a PLQY up to 45% and a carrier lifetime of 5 ns. PNCs were deposited as films on blue-emitting InGaN LEDs and coated with a UV glue, with the purpose being to protect the prepared device against any air-borne contamination and eventual degradation of the perovskite. By measuring the perovskite device into the VLC configuration, a maximum of bandwidth of 700 MHz was reached. A fast radiative recombination dynamic into the nanocrystals is the reason to favor the data travelling at this frequency value. On the other hand, Fu et al. [9] introduced PNCs-PMMA composites, with the perovskites being based on yellow-emitting mixed halide $CsPbBr_{1.5}I_{1.5}$ and red-emitting $CsPbI_3$ nanoparticles. After encapsulation with PMMA, the PL spectra of the nanocrystals were obtained, being stable for around half year under ambient conditions, thus avoiding material degradation (eventual α-to-δ phase transformation). Interestingly, these materials provided enhanced frequency bandwidths of 347 and 822 MHz, respectively, which were much larger than those of traditional phosphors.

Thus, PNCs were suitable for high-speed white-light VLC systems, depositing them on blue GaN μ-LEDs. The corresponding combinations between yellow- and red-emitting active layers with the blue-μ-LEDs produced a warm white emission with a CRI of ~75.7%, a

maximum frequency bandwidth of 1005 MHz, and a real-time data transmission ~1.7 Gbps (Figure 4e,f). These values represent the highest performance reached for LED-based VLC systems thus far, and this response is higher than a previous contribution, where a yellow-emitting $CsPbBr_{1.8}I_{1.2}$ PNCs was analyzed as a potential light converter [13]. Here, the luminescent material deposited on blue-μ-LEDs provided a maximum frequency bandwidth and data rate of ~85 MHz and 300 Mbps, respectively. Differences in (i) the amount of iodide into the nanoparticles requiredto cover longer wavelengths and (ii) the presence of PMMA required to provide stability to the material are possible reasons for obtaining an enhancement in the VLC process.
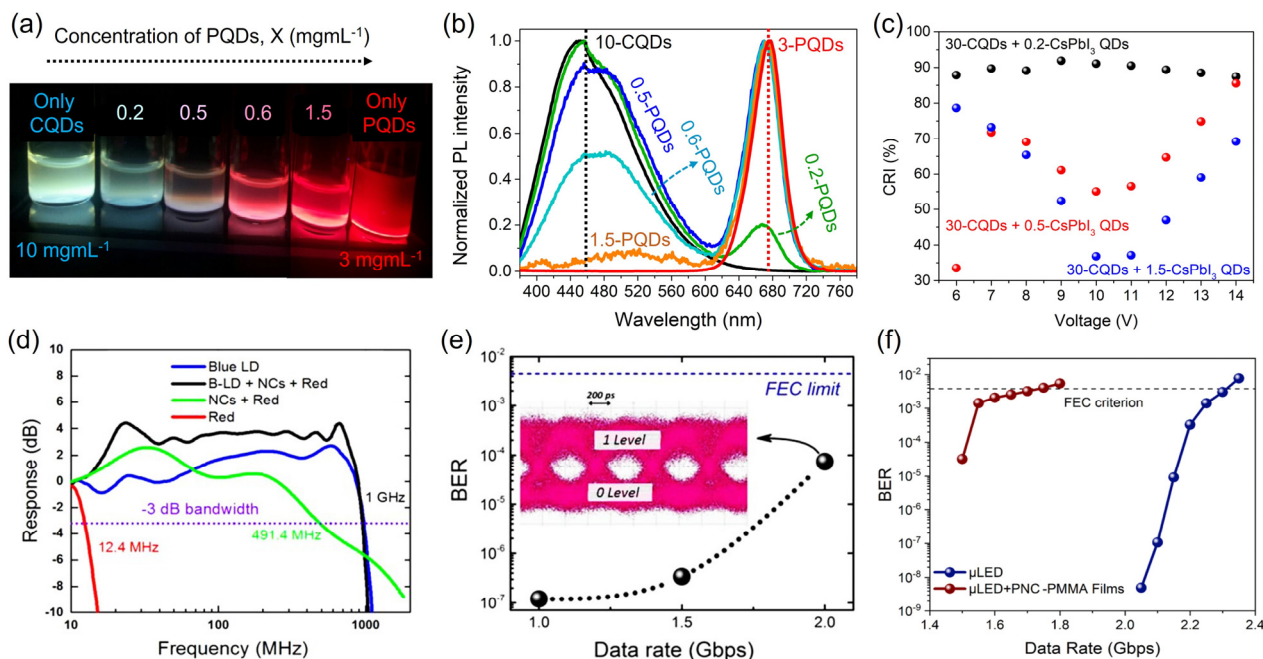
Figure 4. (**a**) Photographs under UV light (λ = 365 nm) and corresponding (**b**) PL spectra of different 10–CQDs-*X*-PNC colloidal solutions, which were generated by varying concentration of perovskite (*X*). (**c**) CRI measurements achieved for 10-CQDs–*X*-PQDs based WLEDs, *X* = 0.2, 0.5, and 1.5. Reproduced under terms of CC–BY license [90]. Copyright 2021, authors, John Wiley and Sons, Inc. (**d**) Frequency response measurements for green- and red-emitting phosphors converters ($CsPbBr_3$ PNCs + nitride phosphor) in absence and presence of commercial blue–LED. (**e**) BERs measurements by varying data rate, applying forward error correction (FEC) limit labeled. Inset of Figure 4e shows eye diagram of 2 Gbit/s data rate where a clear open eye is depicted. Reproduced under terms of CC-BY license [8]. Copyright 2016, Authors. American Chemical Society. (**f**) BERs measurements for air–stable red– and yellow–emitting $CsPb(Br/I)_3$ and $CsPbI_3$ PNCs–PMMA composites (PNCs–PMMA) deposited on a blue-light μLED. BERs was also estimated in absence of light converter for comparative purposes. Reproduced with permission [9]. Copyright 2021, American Chemical Society.

To compare the potentiality of the above-mentioned materials in accelerating wireless data travelling processes, Table 1 summarizes the parameters obtained from the most efficient VLC systems (in terms of estimated frequencies and data rates) depending on the nature of the light converter. Attending to the comparison between the luminescent materials, the combination of organic molecules is a suitable alternative used to achieve a wider frequency bandwidth and, thereby, a higher data rate, due to a favored carrier mobility. Nevertheless, actual records of these parameters were achieved using inorganic systems, such as PNCs, in which a higher absorption coefficient and an easier modulation of their band gap are exhibited through the quantum confinement regime or composition engineering (in this case, the presence of iodide will facilitate the data transmission at longer wavelengths). In this scenario, better color quality in these materials is obtained (related

with high PLQY) as covering a broad range of the UV-vis-NIR spectrum. Thus, recent state-of-the-art developments address the types of devices, diverse architectures, and novel strategies required to improve the way that the data/information is transferred [94,95]. At this point, the rate and capability required to expand the frequency where the communication is travelling is increased. In this actual contribution, we study the most significant luminescent elements, which are the backbone and initial step required to create the suitable integrated system for VLC.

**Table 1.** VLC parameters obtained using different light converters in potential wireless optical systems.

Luminescent Material	PLQY (%)	Integrated System for VLC	Maximum Frequency Bandwidth (MHz)	Data Rate (Mbps)	Ref.
Al-DBA MOF	12	MOF-WLED	3.6	3.6	[27]
Zr-based MOFs	-	MMM	80	215	[29]
BCP and PTCBI	-	OPD	430	-	[58]
Poly p-phenylene vinylene copolymer	60	OVLC	200	1680	[17]
TBPe and BDAVBi	-	OLED	245	1000	[32]
MDMO-PPV	-	PLED	0.27	10	[49]
BBEHP-PPV and MEH-PPV	25	OVLC	200	350	[7]
BODIPY (Y and T-based species)	55–75	OVLC	39	100	[4]
Y-BODIPY	49	OVLC	73	370	[69]
Dialkylfluorene/bicyclic 2,1,3-benzothiadiazole-BODIPY	87–95	OVLC	55	207–218	[72]
$CsPbBr_3$ PNCs	70	Inorganic μ-LED	491	2000	[8]
PMMA-coated $CsPbBr_{1.5}I_{1.5}$ and $CsPbI_3$ PNCs	-	Inorganic μ-LED	1005–1100	1700	[9]
$CsPbBr_{1.8}I_{1.2}$ PNCs	78	Inorganic μ-LED	85	300	[13]

3. Applications of Luminescent Materials in VLC

The preparation PNCs with versatile surface chemistry were adequate for the VLC applications, such as Li-Fi (Light Fidelity) systems, which, unlike conventional Wi-Fi (Wireless Fidelity), are bidirectional wireless communication processes mediated using visible light. A typical Li-Fi system is based on a couple of high quantity of transmitters (LEDs) and signal receivers that match the demand of high-speed wireless communication and multiuser interaction [96,97]. As they make data transference as fast as possible, electroluminescent fibers are the most important communication line between the emitter diode and the receptor in the wireless optical system, offering a high emission color quality and the fabrication of an inexpensive process. Organic materials and polymers were employed as OLEDs to obtain efficient Li-Fi; however, these tools require a high turn-on voltage to mobilize ions into the device, slowing the data transmission. Therefore, the use of PNCs inks represents a low-cost alternative to create light-emitting/detecting bifunctional fibers, as shown in Figure 5a, with narrow electroluminescence linewidth, as shown in Figure 5b,c; as well as creating a small exciton binding energy, which mediates a favored carrier transport to enable the fast travel of information into the wireless tools [97]. As depicted above, LEDs based on orange- or red-light emission develop 0.7–1 GHz modulation bandwidths and a real-time data transmission near to 2 Gbps.

Another type of wireless application is related to the underwater optical communication (UWOC), which attends to the fact that radio frequency suffers from a high attenuation in water, and, therefore, the infrared signal cannot propagate effectively in this medium [98]. In this context, stable underwater emitters with good PL properties, fast radiative recombination pathway and low light attenuation are key factors that influence the transmission distance, frequency bandwidth and data rate [99]. However, the ionic nature of the PNCs

hinders their applicability in polar solvents, causing a rapid quenching of their emission features. In this way, it was reported the introduction of PNCs into the amorphous glass avoided direct interaction between water and the nanoparticles, making them viable for use in a UWOC system [100]. For instance, $CsPbBr_3$ films, as shown in Figure 5d, can provide a PLQY ~69%, which decreases to 53% after 2 weeks in the polar environment. At this point, the high refraction index of the glass accelerates the carrier radiative channel of the perovskite, obtaining a bandwidth of 180 MHz and data rate of 185 Mbps, as shown in Figure 5e,f.
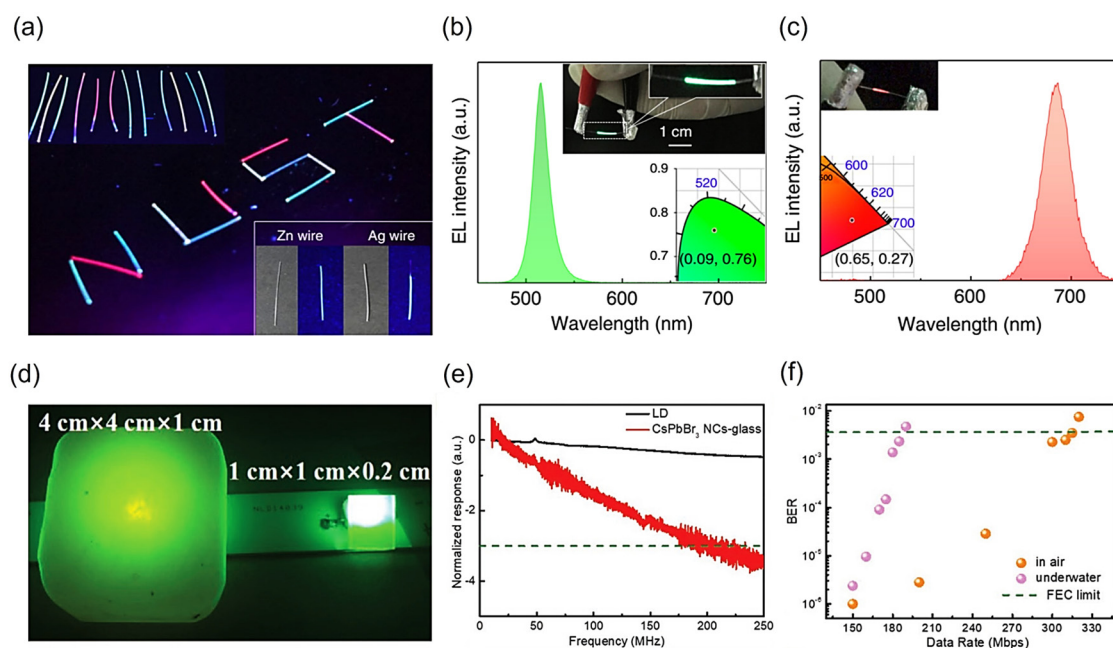
Figure 5. (**a**) Luminescent fibers fabricated from $CsPbI_3$, $CsPbBr_3$ and mixed halide $CsPb(Br/Cl)_3$ inks arranged in a NUST pattern, before being exposed to UV light. Inset of Figure 1a shows emitting PNCs deposited on Zn and Ag wires. Typical electroluminescence (EL) spectra of (**b**) green- and (**c**) red-emitting PNCs fibers. Insets of Figure 5b,c exhibit EL and corresponding chromaticity coordinates of PNCs-based fibers under operation. Reproduced under terms of the CC-BY license [97]. Copyright 2020, Authors, Springer Nature. (**d**) Photograph of green-emitting $CsPbBr_3$ PNCs embedded into amorphous glass at diverse sizes under UV light. (**e**) Frequency response and (**f**) BERs measurements of $CsPbBr_3$–glass material by varying date rate. Reproduced with permission [100]. Copyright 2021, Authors, John Wiley and Sons, Inc.

4. Current Challenges of Using Luminescent Materials for Visible-Light Communication

As we highlighted in the earlier sections, interesting systems, such as MOFs, polymers, complex organic molecules, dyes, and perovskite nanoparticles, are the most promising luminescent materials in terms of making possible the faster transmission and consumption of information/data through VLC compared to the traditional IR-frequency systems. Nevertheless, although these materials exhibit improved PL properties, some issues impede the achievement of a suitable frequency bandwidth and, therefore, the obtainment of an extended response in the UV–vis–NIR spectrum. Firstly, the preparation of some organic molecules or more complex structures, such as MOFs, requires multiple reaction steps, and the amount obtained from these products is usually relatively small, hindering their industrial projection. Moreover, most products do not offer a high PLQY, deducing both that the non-radiative recombination is facilitated (loss of expected emission features) and the PL lifetime of some light converters is in the scale of microseconds. This disadvantage delays the radiative recombination, making it difficult to generate a frequency response at longer wavelengths. Therefore, after depositing visible-light emitters, such as yellow

phosphors on blue-emitting LEDs, the yellow emission is filtered to overpass the long carrier radiative recombination dynamics and accelerate the data travelling. In addition, some issues associated with photobleaching, sensitivity of environmental factors (pH, humidity, temperature, etc.), and a low signal-to-noise ratio hamper the performance of VLCs [101]. Lastly, some organics show low carrier mobility, indicating high capacitance feature, which leads to a lower frequency bandwidth.

Concerning inorganic materials, such as PNCs, iodide-based nanoparticles can suffer an α-to-δ phase transformation [102], quenching their emission properties and any possibility of data mobility via wireless light communication. In this context, future studies should be focused on the preparation of luminescent materials with high PLQY and improved color quality, which can mediate the generation of white light emission by enhancing illumination quality (higher CRI). Besides these characteristics, the PL lifetime response of the materials should be in the range of nanoseconds (1–10 ns), with PNCs being the candidates used to satisfy fast data transmission demand. As reported in optoelectronics and photovoltaics, the confinement effect of the PNCs can avoid the phase transformation in iodide perovskites, opening the door to cover the entire UV-vis-NIR spectrum, accelerating the radiative recombination and expanding the frequency bandwidth. In this line, stable light converters would be incorporated into the actual technologies, such as efficient LEDs for phone and lighting companies, promoting their commercialization.

5. Concluding Remarks

In this review, we highlighted the use of potential light converters with improved PL properties and color quality that are able to cover a wide range from the energy spectrum, thus facilitating data/information diffusion in optical wireless technologies. Mainly, the use of modified MOFs and conjugated polymer structures with modulable emission features (from green to orange-red color) constitutes an ideal option to extend the bandwidth of the data transmission to reach an efficient VLC process. Here, a maximum bandwidth of ~430 MHz and efficient data rate of ~1.6 Mbps were reached. Some limitations related to the lack of commercially available organic compounds with adequate PL properties, as well as the limited number of studies where these improved materials are incorporated as light converters, hindered their use in VLC. On the other hand, OLEDs achieved a significant advancement in their development by introducing conjugated polymer systems. This development increases the carrier mobility into the device, allowing it to obtain a frequency bandwidth and data rate value of 245 MHz and 1 Gbps, respectively. These features promoted the use of another kind of organic compound derived from BODIPY molecules, producing new organic light-emitting devices with white emission, as well as improved color properties, such as CRI of 95% and CCT of 4200 K. Unfortunately, low bandwidth values up to 50 MHz were reached, presenting a disadvantage compared to another light converter used for VLC technologies.

Hence, a third option is the use of PNCs, the PL properties of which can be controlled through composition and particle size engineering (quantum confinement). At this point, the band gap can be modulated, giving a high possibility of obtaining a wider bandwidth for data transfer in VLC processes. Alternatives, such as the combination of cyan-emitting QDs with PNCs used as red-light converters to produce white color emission inks with PLQY ~75%, favor the fabrication of WLEDs with CRI ~95%. On the other hand, it is important to recognize the fact that for the fast radiative recombination dynamics of these nanocrystals, for instance, green-emitting PNCs, a maximum frequency bandwidth of 491.4 MHz were reported, which had one of the highest values achieved for VLC compared to standard phosphor-based converters. Nevertheless, the incorporation of iodide into PNCs to generate mixed halide $CsPbBr_{1.5}I_{1.5}$ and synthesize pure $CsPbI_3$ nanoparticles favors the fabrication of high-speed white-light VLC systems, with a maximum bandwidth of ~1000 MHz and a real-time data transmission of ~1.7 Gbps. Some issues related to the material instability are also evident, with a crystalline phase transformation (α-to-δ phase) quenching the emission features of the perovskite. Here, encapsulation with a PMMA layer

can hinder this transition and preserve the structural integrity of the light converter. From our point of view, the best option to expand the modulation bandwidth of VLC and increase the real-time data rate is through obtaining light converters capable of covering a broad range of the UV-vis-NIR. This outcome means that the coupling of different multicolor and stable luminescent organic species, or the use of confined PNCs with diverse halide composition (tunable band gap), are the most promising materials to provide efficient light-emitting devices that are suitable for future optical wireless applications.

References

1. Khan, L.U.; Yaqoob, I.; Imran, M.; Han, Z.; Hong, C.S. 6G Wireless Systems: A Vision, Architectural Elements, and Future Directions. *IEEE Access* **2020**, *8*, 147029–147044. [CrossRef]
2. Eltokhy, M.A.R.; Abdel-Hady, M.; Haggag, A.; El-Bendary, M.A.M.; Ali, H.; Hosny, T. Audio SIMO system based on visible light communication using cavity LEDs. *Multimed. Tools Appl.* **2023**, 1–15. [CrossRef]
3. Zhang, R.; You, B.; Wang, S.; Han, K.; Shen, X.; Wang, W. Broadband and switchable terahertz polarization converter based on graphene metasurfaces. *Opt. Express* **2021**, *29*, 24804–24815. [CrossRef]
4. Sajjad, M.T.; Manousiadis, P.P.; Orofino, C.; Cortizo-Lacalle, D.; Kanibolotsky, A.L.; Rajbhandari, S.; Amarasinghe, D.; Chun, H.; Faulkner, G.; O'Brien, D.C.; et al. Fluorescent Red-Emitting BODIPY Oligofluorene Star-Shaped Molecules as a Color Converter Material for Visible Light Communications. *Adv. Opt. Mater.* **2015**, *3*, 536–540. [CrossRef]
5. Yu, J.; Wei, Z.; Guan, X.; Zheng, Y.; Zhang, X.; Wang, J.; Wang, S.; Liu, N.; Xu, Y. High-speed real-time visible light communication system based on InGaN/GaN-base multi-quantum well blue micro-LED. *Optoelectron. Lett.* **2021**, *17*, 741–745. [CrossRef]
6. Haggar, J.I.H.; Cai, Y.; Bai, J.; Ghataora, S.; Wang, T. Long-Wavelength Semipolar (11–22) InGaN/GaN LEDs with Multi-Gb/s Data Transmission Rates for VLC. *ACS Appl. Electron. Mater.* **2021**, *3*, 4236–4242. [CrossRef]
7. Sajjad, M.T.; Manousiadis, P.P.; Chun, H.; Vithanage, D.A.; Rajbhandari, S.; Kanibolotsky, A.L.; Faulkner, G.; O'Brien, D.; Skabara, P.J.; Samuel, I.D.W.; et al. Novel Fast Color-Converter for Visible Light Communication Using a Blend of Conjugated Polymers. *ACS Photonics* **2015**, *2*, 194–199. [CrossRef]
8. Dursun, I.; Shen, C.; Parida, M.R.; Pan, J.; Sarmah, S.P.; Priante, D.; Alyami, N.; Liu, J.; Saidaminov, M.I.; Alias, M.S.; et al. Perovskite Nanocrystals as a Color Converter for Visible Light Communication. *ACS Photonics* **2016**, *3*, 1150–1156. [CrossRef]
9. Wang, Z.; Wei, Z.; Cai, Y.; Wang, L.; Li, M.; Liu, P.; Xie, R.; Wang, L.; Wei, G.; Fu, H.Y. Encapsulation-Enabled Perovskite–PMMA Films Combining a Micro-LED for High-Speed White-Light Communication. *ACS Appl. Mater. Interfaces* **2021**, *13*, 54143–54151. [CrossRef]
10. Kang, C.H.; Dursun, I.; Liu, G.; Sinatra, L.; Sun, X.; Kong, M.; Pan, J.; Maity, P.; Ooi, E.-N.; Ng, T.K.; et al. High-speed colour-converting photodetector with all-inorganic CsPbBr3 perovskite nanocrystals for ultraviolet light communication. *Light Sci. Appl.* **2019**, *8*, 1–12. [CrossRef]
11. López-Fraguas, E.; Arredondo, B.; Vega-Colado, C.; Pozo, G.d.; Najafi, M.; Martín-Martín, D.; Galagan, Y.; Sánchez-Pena, J.M.; Vergaz, R.; Romero, B. Visible Light Communication system using an organic emitter and a perovskite photodetector. *Org. Electron.* **2019**, *73*, 292–298. [CrossRef]
12. James Singh, K.; Huang, Y.-M.; Ahmed, T.; Liu, A.-C.; Huang Chen, S.-W.; Liou, F.-J.; Wu, T.; Lin, C.-C.; Chow, C.-W.; Lin, G.-R.; et al. Micro-LED as a Promising Candidate for High-Speed Visible Light Communication. *Appl. Sci.* **2020**, *10*, 7384. [CrossRef]
13. Mei, S.; Liu, X.; Zhang, W.; Liu, R.; Zheng, L.; Guo, R.; Tian, P. High-Bandwidth White-Light System Combining a Micro-LED with Perovskite Quantum Dots for Visible Light Communication. *ACS Appl. Mater. Interfaces* **2018**, *10*, 5641–5648. [CrossRef]
14. Hu, P.; Liu, Y.; Sun, P.; Yao, Q.; Liu, Z.; Luo, Z.; Chao, K.; Jiang, H.; Jiang, J. Tunable YAG:Ce3+ ceramic phosphors for white laser-diode lighting in transmissive/reflective models. *Mater. Res. Bull.* **2021**, *140*, 111297. [CrossRef]
15. Cantarano, A.; Ibanez, A.; Dantelle, G. Garnet-Type Nanophosphors for White LED Lighting. *Front. Mater.* **2020**, *7*, 210. [CrossRef]

16. Zhang, X.; Zhang, D.; Kan, D.; Wu, T.; Song, Y.; Zheng, K.; Sheng, Y.; Shi, Z.; Zou, H. Crystal structure, luminescence properties and application performance of color tuning Y2Mg2Al2Si2O12:Ce3+,Mn2+ phosphors for warm white light-emitting diodes. *Mater. Adv.* **2020**, *1*, 2261–2270. [CrossRef]

17. Hyunchae, C.; Manousiadis, P.; Rajbhandari, S.; Vithanage, D.A.; Faulkner, G.; Tsonev, D.; McKendry, J.J.D.; Videv, S.; Enyuan, X.; Erdan, G.; et al. Visible Light Communication Using a Blue GaN μLED and Fluorescent Polymer Color Converter. *IEEE Photonics Technol. Lett.* **2014**, *26*, 2035–2038. [CrossRef]

18. Zhang, Y.; Xu, R.; Kang, Q.; Zhang, X.; Zhang, Z.-h. Recent Advances on GaN-Based Micro-LEDs. *Micromachines* **2023**, *14*, 991. [CrossRef]

19. Zhao, J.; Yin, Y.; He, R.; Chen, R.; Zhang, S.; Long, H.; Wang, J.; Wei, T. GaN-based parallel micro-light-emitting diode arrays with dual-wavelength InxGa1-xN/GaN MQWs for visible light communication. *Opt. Express* **2022**, *30*, 18461. [CrossRef]

20. Kumar, V.; Kymissis, I. MicroLED/LED electro-optical integration techniques for non-display applications. *Appl. Phys. Rev.* **2023**, *10*, 021306. [CrossRef]

21. Lu, T.; Lin, X.; Guo, W.; Tu, C.-C.; Liu, S.; Lin, C.-J.; Chen, Z.; Kuo, H.-C.; Wu, T. High-speed visible light communication based on micro-LED: A technology with wide applications in next generation communication. *Opto-Electron. Sci.* **2022**, *1*, 220020. [CrossRef]

22. Minotto, A.; Haigh, P.A.; Łukasiewicz, Ł.G.; Lunedei, E.; Gryko, D.T.; Darwazeh, I.; Cacialli, F. Visible light communication with efficient far-red/near-infrared polymer light-emitting diodes. *Light Sci. Appl.* **2020**, *9*, 70. [CrossRef] [PubMed]

23. Manousiadis, P.P.; Yoshida, K.; Turnbull, G.A.; Samuel, I.D.W. Organic semiconductors for visible light communications. *Philos. Trans. R. Soc. A Math. Phys. Eng. Sci.* **2020**, *378*, 20190186. [CrossRef]

24. Zhao, W.; Peng, J.; Wang, W.; Liu, S.; Zhao, Q.; Huang, W. Ultrathin two-dimensional metal-organic framework nanosheets for functional electronic devices. *Coord. Chem. Rev.* **2018**, *377*, 44–63. [CrossRef]

25. Wang, J.; Yu, Y.; Liu, X.; Zhang, Y.; Zhou, X.; Lu, Y. Metal-organic framework based OLED for visible light communication. In Proceedings of the 2019 18th International Conference on Optical Communications and Networks (ICOCN), Huangshan, China, 5–8 August 2019; pp. 1–3.

26. Chen, W.; Zhuang, Y.; Wang, L.; Lv, Y.; Liu, J.; Zhou, T.-L.; Xie, R.-J. Color-Tunable and High-Efficiency Dye-Encapsulated Metal–Organic Framework Composites Used for Smart White-Light-Emitting Diodes. *ACS Appl. Mater. Interfaces* **2018**, *10*, 18910–18917. [CrossRef] [PubMed]

27. Wang, Z.; Wang, Z.; Lin, B.; Hu, X.; Wei, Y.; Zhang, C.; An, B.; Wang, C.; Lin, W. Warm-White-Light-Emitting Diode Based on a Dye-Loaded Metal–Organic Framework for Fast White-Light Communication. *ACS Appl. Mater. Interfaces* **2017**, *9*, 35253–35259. [CrossRef]

28. Pandey, P.; Thapa, K.; Ojha, G.P.; Seo, M.-K.; Shin, K.H.; Kim, S.-W.; Sohn, J.I. Metal-organic frameworks-based triboelectric nanogenerator powered visible light communication system for wireless human-machine interactions. *Chem. Eng. J.* **2023**, *452*, 139209. [CrossRef]

29. Wang, J.-X.; Wang, Y.; Nadinov, I.; Yin, J.; Gutiérrez-Arzaluz, L.; Healing, G.; Alkhazragi, O.; Cheng, Y.; Jia, J.; Alsadun, N.; et al. Metal–Organic Frameworks in Mixed-Matrix Membranes for High-Speed Visible-Light Communication. *J. Am. Chem. Soc.* **2022**, *144*, 6813–6820. [CrossRef]

30. Lustig, W.P.; Shen, Z.; Teat, S.J.; Javed, N.; Velasco, E.; O'Carroll, D.M.; Li, J. Rational design of a high-efficiency, multivariate metal–organic framework phosphor for white LED bulbs. *Chem. Sci.* **2020**, *11*, 1814–1824. [CrossRef]

31. Wang, J.; Ye, F.; Huang, Z.; Zhang, Y.; Zhou, X.; Lu, Y. Linearly polarized surface warm-yellow LED based on orientated organic dyes in rod-like metal-organic framework crystal arrays. *Opt. Mater. Express* **2018**, *8*, 2901–2909. [CrossRef]

32. Yoshida, K.; Manousiadis, P.P.; Bian, R.; Chen, Z.; Murawski, C.; Gather, M.C.; Haas, H.; Turnbull, G.A.; Samuel, I.D.W. 245 MHz bandwidth organic light-emitting diodes used in a gigabit optical wireless data link. *Nat. Commun.* **2020**, *11*, 1171. [CrossRef]

33. Ferreira, R.X.G.; Xie, E.; McKendry, J.J.D.; Rajbhandari, S.; Chun, H.; Faulkner, G.; Watson, S.; Kelly, A.E.; Gu, E.; Penty, R.V.; et al. High Bandwidth GaN-Based Micro-LEDs for Multi-Gb/s Visible Light Communications. *IEEE Photonics Technol. Lett.* **2016**, *28*, 2023–2026. [CrossRef]

34. Wu, T.-C.; Chi, Y.-C.; Wang, H.-Y.; Tsai, C.-T.; Lin, G.-R. Blue Laser Diode Enables Underwater Communication at 12.4 Gbps. *Sci. Rep.* **2017**, *7*, 40480. [CrossRef]

35. Chi, Y.-C.; Hsieh, D.-H.; Lin, C.-Y.; Chen, H.-Y.; Huang, C.-Y.; He, J.-H.; Ooi, B.; DenBaars, S.P.; Nakamura, S.; Kuo, H.-C.; et al. Phosphorous Diffuser Diverged Blue Laser Diode for Indoor Lighting and Communication. *Sci. Rep.* **2015**, *5*, 18690. [CrossRef]

36. Wu, T.; Lin, Y.; Huang, Y.-M.; Liu, M.; Singh, K.J.; Lin, W.; Lu, T.; Zheng, X.; Zhou, J.; Kuo, H.-C.; et al. Highly stable full-color display device with VLC application potential using semipolar μLEDs and all-inorganic encapsulated perovskite nanocrystal. *Photonics Res.* **2021**, *9*, 2132. [CrossRef]

37. Amjad, A.A.; Qasem, Z.; Li, Y.; Li, Q.; Fu, H. All-inorganic liquid phase quantum dots and blue laser diode-based white-light source for simultaneous high-speed visible light communication and high-efficiency solid-state lighting: Publisher's note. *Opt. Express* **2022**, *30*, 35112–35124. [CrossRef]

38. Wu, T.-C.; Chi, Y.-C.; Wang, H.-Y.; Tsai, C.-T.; Huang, Y.-F.; Lin, G.-R. Tricolor R/G/B Laser Diode Based Eye-Safe White Lighting Communication Beyond 8 Gbit/s. *Sci. Rep.* **2017**, *7*, 11. [CrossRef]

39. Tsai, C.-T.; Cheng, C.-H.; Kuo, H.-C.; Lin, G.-R. Toward high-speed visible laser lighting based optical wireless communications. *Prog. Quantum Electron.* **2019**, *67*, 100225. [CrossRef]

40. Chen, H.; Xu, Z.; Gao, Q.; Li, S. A 51.6 Mb/s Experimental VLC System Using a Monochromic Organic LED. *IEEE Photonics J.* **2018**, *10*, 1–12. [CrossRef]

41. Haigh, P.A.; Minotto, A.; Burton, A.; Ghassemlooy, Z.; Murto, P.; Genene, Z.; Mammo, W.; Andersson, M.R.; Wang, E.; Cacialli, F.; et al. Experimental Demonstration of Staggered CAP Modulation for Low Bandwidth Red-Emitting Polymer-LED Based Visible Light Communications. In Proceedings of the 2019 IEEE International Conference on Communications Workshops (ICC Workshops), Shanghai, China, 20–24 May 2019; pp. 1–6. [CrossRef]

42. Le, S.T.; Kanesan, T.; Bausi, F.; Haigh, P.A.; Rajbhandari, S.; Ghassemlooy, Z.; Papakonstantinou, I.; Popoola, W.O.; Burton, A.; Le Minh, H.; et al. 10 Mb/s visible light transmission system using a polymer light-emitting diode with orthogonal frequency division multiplexing. *Opt. Lett.* **2014**, *39*, 3876. [CrossRef]

43. De Souza, P.; Bamiedakis, N.; Yoshida, K.; Manousiadis, P.P.; Turnbull, G.A.; Samuel, I.D.W.; Penty, R.V.; White, I.H. High-Bandwidth Organic Light Emitting Diodes for Ultra-Low Cost Visible Light Communication Links. In Proceedings of the 2018 20th International Conference on Transparent Optical Networks (ICTON), Bucharest, Romania, 1–5 July 2018; pp. 1–4. [CrossRef]

44. Haigh, P.A.; Bausi, F.; Le Minh, H.; Papakonstantinou, I.; Popoola, W.O.; Burton, A.; Cacialli, F. Wavelength-Multiplexed Polymer LEDs: Towards 55 Mb/s Organic Visible Light Communications. *IEEE J. Sel. Areas Commun.* **2015**, *33*, 1819–1828. [CrossRef]

45. Gelkop, B.; Aichnboim, L.; Malka, D. RGB wavelength multiplexer based on polycarbonate multicore polymer optical fiber. *Opt. Fiber Technol.* **2021**, *61*, 102441. [CrossRef]

46. Zampetti, A.; Minotto, A.; Cacialli, F. Near-Infrared (NIR) Organic Light-Emitting Diodes (OLEDs): Challenges and Opportunities. *Adv. Funct. Mater.* **2019**, *29*, 1807623. [CrossRef]

47. Minotto, A.; Murto, P.; Genene, Z.; Zampetti, A.; Carnicella, G.; Mammo, W.; Andersson, M.R.; Wang, E.; Cacialli, F. Efficient Near-Infrared Electroluminescence at 840 nm with "Metal-Free" Small-Molecule:Polymer Blends. *Adv. Mater.* **2018**, *30*, 1706584. [CrossRef]

48. Park, J. Speedup of Dynamic Response of Organic Light-Emitting Diodes. *J. Light. Technol.* **2010**, *28*, 2873–2880. [CrossRef]

49. Haigh, P.A.; Bausi, F.; Ghassemlooy, Z.; Papakonstantinou, I.; Le Minh, H.; Fléchon, C.; Cacialli, F. Visible light communications: Real time 10 Mb/s link with a low bandwidth polymer light-emitting diode. *Opt. Express* **2014**, *22*, 2830. [CrossRef]

50. Haigh, P.A.; Ghassemlooy, Z.; Le Minh, H.; Rajbhandari, S.; Arca, F.; Tedde, S.F.; Hayden, O.; Papakonstantinou, I. Exploiting Equalization Techniques for Improving Data Rates in Organic Optoelectronic Devices for Visible Light Communications. *J. Light. Technol.* **2012**, *30*, 3081–3088. [CrossRef]

51. Chun, H.; Chiang, C.-J.; Monkman, A.; O'Brien, D. A Study of Illumination and Communication using Organic Light Emitting Diodes. *J. Light. Technol.* **2013**, *31*, 3511–3517. [CrossRef]

52. Haigh, P.A.; Ghassemlooy, Z.; Zvánovec, S.; Komanec, M. VLC with Organic Photonic Components. In *Visible Light Communications*; Routledge Handbooks Online; CRC Press: Boca Raton, FL, USA, 2017; pp. 521–548. [CrossRef]

53. Clark, J.; Lanzani, G. Organic photonics for communications. *Nat. Photonics* **2010**, *4*, 438–446. [CrossRef]

54. Tang, C.W.; VanSlyke, S.A. Organic electroluminescent diodes. *Appl. Phys. Lett.* **1987**, *51*, 913–915. [CrossRef]

55. Thejokalyani, N.; Dhoble, S.J. Novel approaches for energy efficient solid state lighting by RGB organic light emitting diodes—A review. *Renew. Sustain. Energy Rev.* **2014**, *32*, 448–467. [CrossRef]

56. Chen, H.; Xu, Z. OLED Panel Radiation Pattern and Its Impact on VLC Channel Characteristics. *IEEE Photonics J.* **2018**, *10*, 1–10. [CrossRef]

57. Baeg, K.-J.; Binda, M.; Natali, D.; Caironi, M.; Noh, Y.-Y. Organic Light Detectors: Photodiodes and Phototransistors. *Adv. Mater.* **2013**, *25*, 4267–4295. [CrossRef]

58. Peumans, P.; Bulović, V.; Forrest, S.R. Efficient, high-bandwidth organic multilayer photodetectors. *Appl. Phys. Lett.* **2000**, *76*, 3855–3857. [CrossRef]

59. Cho, S.; Heo, C.J.; Lim, Y.; Oh, S.; Minami, D.; Yu, M.; Chun, H.; Yun, S.; Seo, H.; Fang, F.; et al. Small Molecule Based Organic Photo Signal Receiver for High-Speed Optical Wireless Communications. *Adv. Sci.* **2022**, *9*, 2203715. [CrossRef]

60. Burroughes, J.H.; Bradley, D.D.C.; Brown, A.R.; Marks, R.N.; Mackay, K.; Friend, R.H.; Burns, P.L.; Holmes, A.B. Light-emitting diodes based on conjugated polymers. *Nature* **1990**, *347*, 539–541. [CrossRef]

61. Uoyama, H.; Goushi, K.; Shizu, K.; Nomura, H.; Adachi, C. Highly efficient organic light-emitting diodes from delayed fluorescence. *Nature* **2012**, *492*, 234–238. [CrossRef]

62. Wang, Q.; Aziz, H. Degradation of Organic/Organic Interfaces in Organic Light-Emitting Devices due to Polaron–Exciton Interactions. *ACS Appl. Mater. Interfaces* **2013**, *5*, 8733–8739. [CrossRef]

63. Apolo, J.A.; Ortega, B.; Almenar, V. Hybrid POF/VLC Links Based on a Single LED for Indoor Communications. *Photonics* **2021**, *8*, 254. [CrossRef]

64. Salamandra, L.; La Notte, L.; Fazolo, C.; Di Natali, M.; Penna, S.; Mattiello, L.; Cinà, L.; Del Duca, R.; Reale, A. A comparative study of organic photodetectors based on P3HT and PTB7 polymers for visible light communication. *Org. Electron.* **2020**, *81*, 105666. [CrossRef]

65. Dadabayev, R.; Malka, D. A visible light RGB wavelength demultiplexer based on polycarbonate multicore polymer optical fiber. *Opt. Laser Technol.* **2019**, *116*, 239–245. [CrossRef]

66. Zhao, G.; Dai, H.; Zhou, R.; Zhang, G.; Chen, H.; Ma, D.; Tian, W.; Ban, X.; Jiang, W.; Sun, Y. Endowing deep-red BODIPY luminophors with enhanced aggregation-induced emission by installing miniature rotor of trifluoromethyl for solution-processed OLEDs. *Org. Electron.* **2022**, *106*, 106530. [CrossRef]

67. Dwivedi, B.K.; Singh, V.D.; Kumar, Y.; Pandey, D.S. Photophysical properties of some novel tetraphenylimidazole derived BODIPY based fluorescent molecular rotors. *Dalton Trans.* **2020**, *49*, 438–452. [CrossRef] [PubMed]

68. Wang, Y.; Wang, Y.; Chi, N.; Yu, J.; Shang, H. Demonstration of 575-Mb/s downlink and 225-Mb/s uplink bi-directional SCM-WDM visible light communication using RGB LED and phosphor-based LED. *Opt. Express* **2013**, *21*, 1203–1208. [CrossRef]

69. Vithanage, D.A.; Manousiadis, P.P.; Sajjad, M.T.; Rajbhandari, S.; Chun, H.; Orofino, C.; Cortizo-Lacalle, D.; Kanibolotsky, A.L.; Faulkner, G.; Findlay, N.J.; et al. BODIPY star-shaped molecules as solid state colour converters for visible light communications. *Appl. Phys. Lett.* **2016**, *109*, 013302. [CrossRef]

70. Sajjad, M.T.; Manousiadis, P.P.; Orofino, C.; Kanibolotsky, A.L.; Findlay, N.J.; Rajbhandari, S.; Vithanage, D.A.; Chun, H.; Faulkner, G.E.; O'Brien, D.C.; et al. A saturated red color converter for visible light communication using a blend of star-shaped organic semiconductors. *Appl. Phys. Lett.* **2017**, *110*, 013302. [CrossRef]

71. Yuce, H.; Guner, T.; Dartar, S.; Kaya, B.U.; Emrullahoglu, M.; Demir, M.M. BODIPY-based organic color conversion layers for WLEDs. *Dye. Pigment.* **2020**, *173*, 107932. [CrossRef]

72. Merkushev, D.A.; Usoltsev, S.D.; Marfin, Y.S.; Pushkarev, A.P.; Volyniuk, D.; Grazulevicius, J.V.; Rumyantsev, E.V. BODIPY associates in organic matrices: Spectral properties, photostability and evaluation as OLED emitters. *Mater. Chem. Phys.* **2017**, *187*, 104–111. [CrossRef]

73. Ma, D.; Zhao, G.; Chen, H.; Zhou, R.; Zhang, G.; Tian, W.; Jiang, W.; Sun, Y. Creation of BODIPYs-based red OLEDs with high color purity via modulating the energy gap and restricting rotation of substituents. *Dye. Pigment.* **2022**, *203*, 110377. [CrossRef]

74. Nakano, T.; Fujikawa, S. Aryl/Heteroaryl Substituted Boron-Difluoride Complexes Bearing 2-(Isoquinol-1-yl)pyrrole Ligands Exhibiting High Luminescence Efficiency with a Large Stokes Shift. *J. Org. Chem.* **2022**, *87*, 11708–11721. [CrossRef]

75. Virgili, T.; Ganzer, L.; Botta, C.; Squeo, B.M.; Pasini, M. Asymmetric AZA-BODIPY with Optical Gain in the Near-Infrared Region. *Molecules* **2022**, *27*, 4538. [CrossRef]

76. De Roo, J.; Ibáñez, M.; Geiregat, P.; Nedelcu, G.; Walravens, W.; Maes, J.; Martins, J.C.; Van Driessche, I.; Kovalenko, M.V.; Hens, Z. Highly Dynamic Ligand Binding and Light Absorption Coefficient of Cesium Lead Bromide Perovskite Nanocrystals. *ACS Nano* **2016**, *10*, 2071–2081. [CrossRef]

77. Jancik Prochazkova, A.; Salinas, Y.; Yumusak, C.; Scharber, M.C.; Brüggemann, O.; Weiter, M.; Sariciftci, N.S.; Krajcovic, J.; Kovalenko, A. Controlling Quantum Confinement in Luminescent Perovskite Nanoparticles for Optoelectronic Devices by the Addition of Water. *ACS Appl. Nano Mater.* **2020**, *3*, 1242–1249. [CrossRef]

78. Lee, C.; Shin, Y.; Villanueva-Antoli, A.; Das Adhikari, S.; Rodríguez-Pereira, J.; Macak, J.M.; Mesa, C.; Yoon, S.J.; Gualdrón-Reyes, A.F.; Mora Seró, I. Efficient and Stable Blue- and Red-Emitting Perovskite Nanocrystals through Defect Engineering: PbX2 Purification. *Chem. Mater.* **2021**, *33*, 8745–8757. [CrossRef]

79. Grisorio, R.; Di Clemente, M.E.; Fanizza, E.; Allegretta, I.; Altamura, D.; Striccoli, M.; Terzano, R.; Giannini, C.; Irimia-Vladu, M.; Suranna, G.P. Exploring the surface chemistry of cesium lead halide perovskite nanocrystals. *Nanoscale* **2019**, *11*, 986–999. [CrossRef]

80. Protesescu, L.; Yakunin, S.; Bodnarchuk, M.I.; Krieg, F.; Caputo, R.; Hendon, C.H.; Yang, R.X.; Walsh, A.; Kovalenko, M.V. Nanocrystals of Cesium Lead Halide Perovskites (CsPbX3, X = Cl, Br, and I): Novel Optoelectronic Materials Showing Bright Emission with Wide Color Gamut. *Nano Lett.* **2015**, *15*, 3692–3696. [CrossRef]

81. Kim, J.S.; Heo, J.-M.; Park, G.-S.; Woo, S.-J.; Cho, C.; Yun, H.J.; Kim, D.-H.; Park, J.; Lee, S.-C.; Park, S.-H.; et al. Ultra-bright, efficient and stable perovskite light-emitting diodes. *Nature* **2022**, *611*, 688–694. [CrossRef]

82. Hao, M.; Bai, Y.; Zeiske, S.; Ren, L.; Liu, J.; Yuan, Y.; Zarrabi, N.; Cheng, N.; Ghasemi, M.; Chen, P.; et al. Ligand-assisted cation-exchange engineering for high-efficiency colloidal Cs1–xFAxPbI3 quantum dot solar cells with reduced phase segregation. *Nat. Energy* **2020**, *5*, 79–88. [CrossRef]

83. Gualdrón-Reyes, A.F.; Masi, S.; Mora-Seró, I. Progress in halide-perovskite nanocrystals with near-unity photoluminescence quantum yield. *Trends Chem.* **2021**, *3*, 499–511. [CrossRef]

84. Bodnarchuk, M.I.; Boehme, S.C.; ten Brinck, S.; Bernasconi, C.; Shynkarenko, Y.; Krieg, F.; Widmer, R.; Aeschlimann, B.; Günther, D.; Kovalenko, M.V.; et al. Rationalizing and Controlling the Surface Structure and Electronic Passivation of Cesium Lead Halide Nanocrystals. *ACS Energy Lett.* **2018**, *4*, 63–74. [CrossRef]

85. Gao, Z.; Wang, X.; Bai, Y.; Sun, C.; Liu, H.; Wang, L.; Su, S.; Tian, K.; Zhang, Z.-H.; Bi, W. High color rendering index and stable white light emitting diodes fabricated from lead bromide perovskites. *Appl. Phys. Lett.* **2019**, *115*, 153103. [CrossRef]

86. Su, Y.; Jing, Q.; Xu, Y.; Xing, X.; Lu, Z. Preventing Anion Exchange between Perovskite Nanocrystals by Confinement in Porous SiO2 Nanobeads. *ACS Omega* **2019**, *4*, 22209–22213. [CrossRef] [PubMed]

87. Gao, Z.; Sun, C.; Liu, H.; Shi, S.; Geng, C.; Wang, L.; Su, S.; Tian, K.; Zhang, Z.-h.; Bi, W. White light-emitting diodes based on carbon dots and Mn-doped CsPbCl3 nanocrystals. *Nanotechnology* **2019**, *30*, 245201. [CrossRef] [PubMed]

88. Zheng, Y.; Yuan, X.; Yang, J.; Li, Q.; Yang, X.; Fan, Y.; Li, H.; Liu, H.; Zhao, J. Cu doping-enhanced emission efficiency of Mn2+ in cesium lead halide perovskite nanocrystals for efficient white light-emitting diodes. *J. Lumin.* **2020**, *227*, 117586. [CrossRef]

89. Shi, E.; Gao, Y.; Finkenauer, B.P.; Akriti; Coffey, A.H.; Dou, L. Two-dimensional halide perovskite nanomaterials and heterostructures. *Chem. Soc. Rev.* **2018**, *47*, 6046–6072. [CrossRef]

90. Rad, R.R.; Gualdrón-Reyes, A.F.; Masi, S.; Ganji, B.A.; Taghavinia, N.; Gené-Marimon, S.; Palomares, E.; Mora-Seró, I. Tunable Carbon–CsPbI3 Quantum Dots for White LEDs. *Adv. Opt. Mater.* **2020**, *9*, 2001508. [CrossRef]

91. Saeedi, M.; Ashjari, T.; Roghabadi, F.A.; Ahmadi, V. Efficient LED Light Converter based on Perovskite Nanocrystals for Visible Light Communication. In Proceedings of the 2020 3rd West Asian Symposium on Optical and Millimeter-Wave Wireless Communication (WASOWC), Tehran, Iran, 24–25 November 2020; pp. 1–4.
92. Li, X.; Ma, W.; Liang, D.; Cai, W.; Zhao, S.; Zang, Z. High-performance CsPbBr3@Cs4PbBr6/SiO2 nanocrystals via double coating layers for white light emission and visible light communication. *eScience* **2022**, *2*, 646–654. [CrossRef]
93. Ma, Z.; Li, X.; Zhang, C.; Turyanska, L.; Lin, S.; Xi, X.; Li, J.; Hu, T.; Wang, J.; Patanè, A.; et al. CsPb(Br/I)3 Perovskite Nanocrystals for Hybrid GaN-Based High-Bandwidth White Light-Emitting Diodes. *ACS Appl. Nano Mater.* **2021**, *4*, 8383–8389. [CrossRef]
94. Geng, Z.; Khan, F.N.; Guan, X.; Dong, Y. Advances in Visible Light Communication Technologies and Applications. *Photonics* **2022**, *9*, 893. [CrossRef]
95. Yu, T.-C.; Huang, W.-T.; Lee, W.-B.; Chow, C.-W.; Chang, S.-W.; Kuo, H.-C. Visible Light Communication System Technology Review: Devices, Architectures, and Applications. *Crystals* **2021**, *11*, 1098. [CrossRef]
96. Hussain, G.K.J.; Shruthe, M.; Rithanyaa, S.; Madasamy, S.R.; Velu, N.S. Visible Light Communication using Li-Fi. In Proceedings of the 2022 6th International Conference on Devices, Circuits and Systems (ICDCS), Coimbatore, India, 21–22 April 2022; pp. 257–262.
97. Shan, Q.; Wei, C.; Jiang, Y.; Song, J.; Zou, Y.; Xu, L.; Fang, T.; Wang, T.; Dong, Y.; Liu, J.; et al. Perovskite light-emitting/detecting bifunctional fibres for wearable LiFi communication. *Light Sci. Appl.* **2020**, *9*, 163. [CrossRef]
98. Ali, M.F.; Jayakody, D.N.K.; Li, Y. Recent Trends in Underwater Visible Light Communication (UVLC) Systems. *IEEE Access* **2022**, *10*, 22169–22225. [CrossRef]
99. Li, X.; Tong, Z.; Lyu, W.; Chen, X.; Yang, X.; Zhang, Y.; Liu, S.; Dai, Y.; Zhang, Z.; Guo, C.; et al. Underwater quasi-omnidirectional wireless optical communication based on perovskite quantum dots. *Opt. Express* **2022**, *30*, 1709–1722. [CrossRef]
100. Xia, M.; Zhu, S.; Luo, J.; Xu, Y.; Tian, P.; Niu, G.; Tang, J. Ultrastable Perovskite Nanocrystals in All-Inorganic Transparent Matrix for High-Speed Underwater Wireless Optical Communication. *Adv. Opt. Mater.* **2021**, *9*, 2002239. [CrossRef]
101. Rybczynski, P.; Smolarkiewicz-Wyczachowski, A.; Piskorz, J.; Bocian, S.; Ziegler-Borowska, M.; Kędziera, D.; Kaczmarek-Kędziera, A. Photochemical Properties and Stability of BODIPY Dyes. *Int. J. Mol. Sci.* **2021**, *22*, 6735. [CrossRef]
102. Yin, Y.; Cheng, H.; Tian, W.; Wang, M.; Yin, Z.; Jin, S.; Bian, J. Self-Assembled δ-CsPbI3 Nanowires for Stable White Light Emission. *ACS Applied Nano Materials* **2022**, *5*, 18879–18884. [CrossRef]